Evidence from EELS of Oxygen in the Nucleation Layer of a MBE grown III-N HEMT

Tyler J. Eustis[1], John Silcox[2], Michael J. Murphy[3], and William J. Schaff[3]
[1]Department of Materials Science and Engineering, Cornell University, Ithaca, NY 14853
[2]School of Applied Engineering Physics, Cornell University, Ithaca, NY 14853
[3]School of Electrical Engineering, Cornell University, Ithaca, NY 14853

ABSTRACT

The presence of oxygen throughout the nominally AlN nucleation layer of a RF assisted MBE grown III-N HEMT was revealed upon examination by Electron Energy Loss Spectroscopy (EELS) in a Scanning Transmission Electron Microscope (STEM). The nucleation layer generates the correct polarity (gallium face) required for producing a piezoelectric induced high mobility two dimensional electron gas at the AlGaN/GaN heterojunction. Only AlN or AlGaN nucleation layers have provided gallium face polarity in RF assisted MBE grown III-N's on sapphire. The sample was grown at Cornell University in a Varian GenII MBE using an EPI Uni-Bulb nitrogen plasma source. The nucleation layer was examined in the Cornell University STEM using Annular Dark Field (ADF) imaging and Parallel Electron Energy Loss Spectroscopy (PEELS). Bright Field TEM reveals a relatively crystallographically sharp interface, while the PEELS reveal a chemically diffuse interface. PEELS of the nitrogen and oxygen K-edges at approximately 5-Angstrom steps across the GaN/AlN/sapphire interfaces reveals the presence of oxygen in the AlN nucleation layer. The gradient suggests that the oxygen has diffused into the nucleation region from the sapphire substrate forming this oxygen containing AlN layer. Based on energy loss near edge structure (ELNES), oxygen is in octahedral interstitial sites in the AlN and Al is both tetrahedrally and octahedrally coordinated in the oxygen rich region of the AlN.

INTRODUCTION

Within the last decade, the III-N semiconductors have experienced rapid development to the point that commercial optical devices are now available. Recently the importance of the piezoelectric properties of the III-N has come to light. With this realization, the knowledge and control of the polarity of III-N thin films has become paramount for device design. The piezoelectric and spontaneous polarizations in this system are large enough to induce a two-dimensional electron gas (2DEG) at $Al_{1-x}Ga_xN$/GaN heterojunctions [1-7]. For Molecular Beam Epitaxy (MBE) material grown on sapphire substrates using a plasma nitrogen source, the nucleation layer determines the polarity of the resulting layers [8]. With this control of the polarity of the material, high quality MBE High Electron Mobility Transistor (HEMT) devices have been achieved [8]. In this paper, the composition and structure of the AlN nucleation layer in a HEMT device structure studied in the Cornell University Scanning Transmission Electron Microscope (STEM), will be presented.

The Cornell University STEM produces an electron probe approximately 2.1Å in diameter and thus is distinctly qualified for near atomic resolution interface

https://doi.org/10.1557/S1092578300004269 Published online by Cambridge University Press

investigations. As this probe is scanned across a TEM type sample, the scattered electrons are collected. Electrons scattered to high angles are collected by the Annular Dark Field (ADF) detector producing an image where the contrast depends mainly on atomic number (Z) and thickness. Thus ADF imaging is commonly referred to as Z-contrast imaging. Electrons scattered to small angles are either detected by the Bright Field Detector, producing an image analogous to normal bright field TEM, or are recorded as EELS by either the Serial or Parallel detector.

EELS provides information about the local bonding and electronic structure by probing unoccupied electronic states. The fast moving electrons from the STEM probe interact with the core electrons in the specimen, which are excited from their ground state to unoccupied states. Since the energy lost by the fast moving electrons in the probe is equal to the difference in energy between the core level and excited level, the measurement of the intensity of the probe electrons as a function of energy loss provides substantial details of the electronic structure and chemistry.

EXPERIMENTAL DETAILS

The III-N HEMT sample with an AlN nucleation layer was grown in a Varian GenII MBE at Cornell University. The specifics of the growth conditions, electrical characterization, and device results are given elsewhere [8]. The sample was prepared by standard tripod polishing techniques to form a wedge specimen [9]. The sample was ion milled with a BAL-TEC Res 010 for final thinning.

The Cornell University STEM has a maximum energy resolution of ~0.7eV over a large energy range (from 0 to 2keV). With high spatial and energy resolution, the STEM is particularly suited for sub-nanometer chemical and structural studies. With such a focused small probe, high spatial resolution EELS can be obtained. Thus compositional and structural information can be acquired with core-loss EELS. In addition, thickness information can be obtained on a nanometer scale from the ratio of the first plasmon intensity to the zero loss (electrons that have lost no energy) intensity. More detailed information concerning the STEM can be found elsewhere.

EELS spectra were acquired using the Parallel EELS detector. Specifically the nitrogen and oxygen K-edges were obtained simultaneously and individually by stepping across the GaN/AlN/Sapphire interfaces. The K-edges correspond to transitions from atomic 1s states to empty local and conduction band states with p-character. Spectra of the aluminum L_{23}-edge were also obtained. The L-edge corresponds to transitions from atomic 2p to empty local and conduction band states with d and s-character. The ADF signal is acquired in conjunction with the spectra. In addition, ADF images of the area of interest collected before and after spectrum acquisition indicated no significant spatial drift.

All data and images are acquired digitally. After acquisition, the spectra were smoothed and shot noise was removed. The background was subtracted using a standard power-law curve fit to the pre-edge. The intensities of the nitrogen and oxygen K-edges were integrated over 50 eV starting at threshold. Ratios of O/N+O were obtained using the standard equation involving integrated intensities and cross section [10]. Acquisition times for the K-edges were selected in an attempt to balance electron beam damage [11] and signal to noise. Thus, for the acquisition times used, some beam damage was

https://doi.org/10.1557/S1092578300004269 Published online by Cambridge University Press

observed in the sapphire substrate. The damage results in a very small artificial nitrogen signal in the sapphire.

DISCUSSION

The presence of oxygen is observed in the AlN nucleation layer upon examination of Figure 1. The oxygen signal is constant within the sapphire substrate. Moving across the AlN/sapphire interface (based on the ADF image in Figure 1(a)), the oxygen signal drops sharply. Once across the interface, the oxygen signal decays and reaches zero at approximately the AlN/GaN interface.

As stated above, the nitrogen signal within the sapphire results from beam damage. Therefore the ratio depicted in Figure 1(c) does not level off at one in the sapphire. On moving from the sapphire to the AlN, the nitrogen signal increases but does not peak until about half way through the AlN, as seen in Figure 1(b).

Upon calculation of the O/O+N ratio using the data in Figure 1(b), thickness effects are removed. The ratio is displayed in Figure 1(c). The ratio decreases at points moving across the AlN/sapphire as the oxygen signal decreases and the nitrogen signal increases.

Figure 2 is a bright field TEM image of the AlN/sapphire interface. The interface

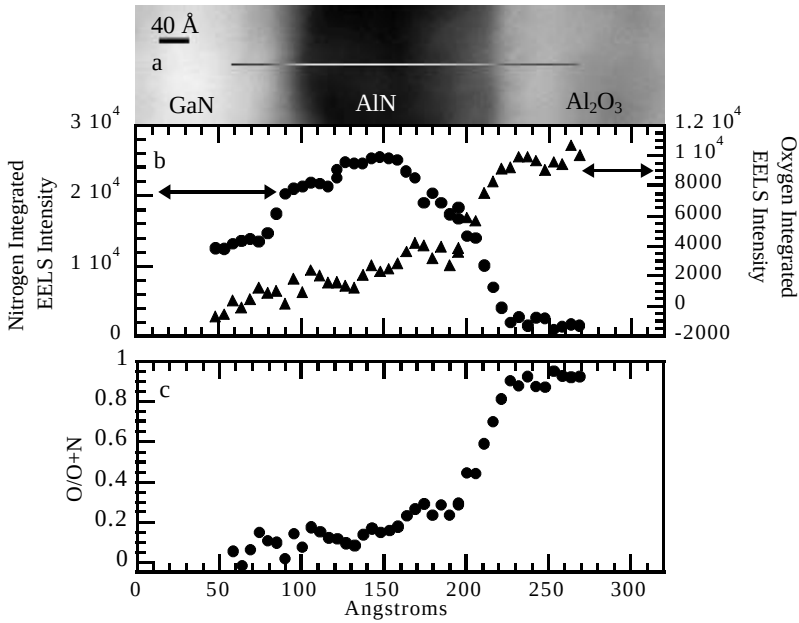

Figure 1. *(a) ADF image of the area of interest. (b) Integrated Intensity of N and O K-edge. (c) The ratio O/O+N vs. distance. The horizontal line represents where the data in (b) and (c) were taken.*

https://doi.org/10.1557/S1092578300004269 Published online by Cambridge University Press

appears fairly abrupt giving no indication of any oxygen containing AlN. Thus un-calibrated bright field TEM imaging is inadequate to detect chemical profiles. Only through strict control of experimental conditions, has chemical mapping of semiconductor interfaces been achieved using bright field TEM images [12]. Others have stated based on TEM images that their observed interface is chemically sharp [13]. Without microanalysis, such claims are difficult to substantiate.

Now we turn to examination of the ELNES in an attempt to learn about the local environment of the individual constituents. Core-loss edges at significant points across the AlN/sapphire interface are displayed in Figure 3. The N K-edge in the oxygen poor AlN and in the oxygen rich AlN are displayed in Figure 3(a). The N K-edge for AlN compares well with previously published spectrum [11]. In Figure 3(a), notice the decrease in intensity of the first peak of the N K-edge from the oxygen rich region of the AlN relative to the other peaks as compared to the N K-edge from the relatively pure AlN. Based on the comparison of the two N K-edges with Multiple Scattering calculations, some of the oxygen in the AlN is in octahedral interstitial positions within the AlN lattice [11]. Abaidia et. al. determined the location of oxygen in AlN based on examination of extended energy loss fine structure. It was determined that oxygen would be in octahedral interstitial sides for Al/(N+O) 0.8 and in substitution positions for Al/(N+O) 1 [14]. Others determined the O in AlN was in substitution sites based on X-ray Absorption Spectroscopy [15]. The possibility of oxygen substituted for nitrogen in the AlN nucleation layer of the HEMT sample examined here cannot be ruled out. Unfortunately no core edge spectroscopy simulations of oxygen substituted for nitrogen are available with which to compare. In addition, it is important to note that the oxygen containing AlN layers examined by the above mentioned groups were grown in an oxygen-containing environment.

Small variations in the O K-edges were observed. However, little information is gained and thus will not be presented here.

Aluminum L-edges are presented and labeled in Figure 3(b). The edges obtained in AlN and in Al_2O_3 match well with published data [11,16]. The Al L-edge obtained at the interface between the AlN and the sapphire is a combination of the edges from AlN and Al_2O_3. In fact, the Al L-edges obtained by stepping across the interface using the parallel EELS detector were a smooth transition from the AlN Al L-edge to the Al_2O_3 Al L-edge. The edge displayed in Figure 3(b) was obtained at the AlN/Al_2O_3 interface. Calculations

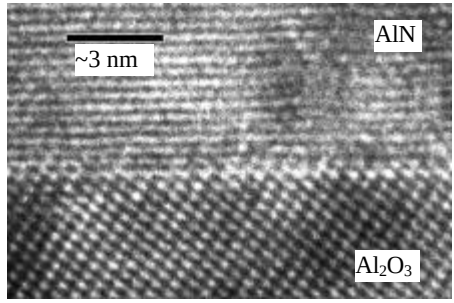

Figure 2. *Bright Field TEM image of the AlN/sapphire interface.*

https://doi.org/10.1557/S1092578300004269 Published online by Cambridge University Press

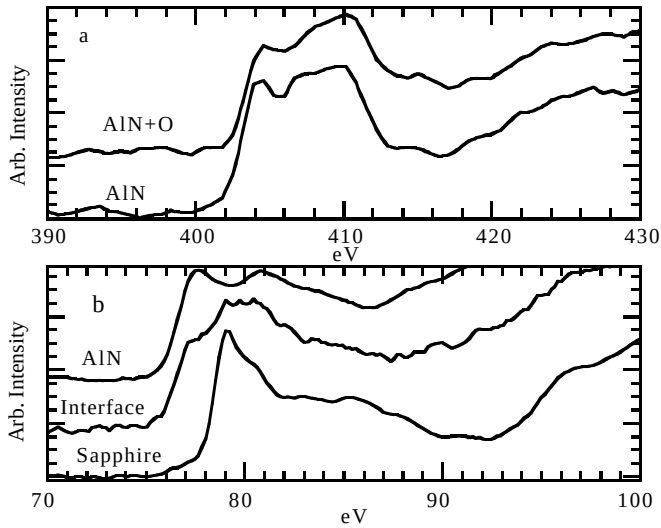

Figure 3. *EELS core-loss edges. (a) The N K-edge in the AlN and at the AlN/sapphire interface. (b) The Al L_{23}-edge in the AlN, at the AlN/sapphire interface, and in the sapphire.*

by Brydson et al. [17] confirm the validity of simply performing a linear sum of Al L-edges to determine the mount of different components. Thus, the Al at the interface is approximately 72% tetrahedrally bonded Al and 28% octahedrally bonded Al.

CONCLUSION

Oxygen has been observed by EELS in the AlN nucleation of a high quality MBE grown III-N HEMT device. The AlN nucleation layer is key to obtaining MBE Ga-face polarity material on sapphire. The oxygen appears to have diffused in from the sapphire substrate. The concentration profile suggests a sharp drop in oxygen crossing the AlN/sapphire interface. Once across the interface, the oxygen concentration decays approaching the GaN/AlN interface. Examination and comparison of the ELNES of the N K-edge and the Al L-edge reveals that oxygen in the AlN is in octahedral interstitial sites and that Al in the oxygen rich region of the AlN has both tetrahedral and octahedral coordination. Bright field TEM images fail to identify a chemical difference in the AlN. Although some information has been gained about the Ga-face polarity determining AlN nucleation layer, it is unclear at this point what role the oxygen plays.

https://doi.org/10.1557/S1092578300004269 Published online by Cambridge University Press

ACKNOWLEDGEMENTS

This work was supported by the Office of Naval Research under MURI Contract No. N00014-96-1-1223 monitored by Dr. John C. Zolper. The Cornell STEM was acquired through the NSF (grant # DMR8314255) and is operated by the Cornell Center for Materials Research (NSF grant #DMR-9632275). The authors would like to acknowledge Mick Thomas and Dr. Earl Kirkland for technical support and helpful discussions.

REFERENCE

1. A. Hangleiter, I. Jin Seo, H. Kollmer, S. Heppel, J. Off, and F. Scholz, MRS Internet Journal of Nitride Semiconductor Research, **3** (15)**, (**1998).
2. P. M. Asbeck, E. T. Yu, S. S. Lau, G. J. Sullivan, J. Van Hove, and J. Redwing, Electronics Letters, **33,** 1230-1, (1997).
3. F. Bernardini, V. Fiorentini, and D. Vanderbilt, Physical Review B, **56,** R10024-7, (1997).
4. A. D. Bykhovski, B. L. Gelmont, and M. S. Shur, Journal of Applied Physics, **81,** 6332-8, (1997).
5. M. B. Nardelli, K. Rapcewicz, and J. Bernholc, Applied Physics Letters, **71,** 3135-7, (1997).
6. T. Takeuchi, H. Takeuchi, S. Sota, H. Sakai, H. Amano, and I. Akasaki, Japanese Journal of Applied Physics, Part 2, **36,** L177-9, (1997).
7. E. T. Yu, G. J. Sullivan, P. M. Asbeck, C. D. Wang, D. Qiao, and S. S. Lau, Applied Physics Letters, **71,** 2794-6, (1997).
8. M. J. Murphy, K. Chu, H. Wu, W. Yeo, W. J. Schaff, O. Ambacher, J. Smart, J. R. Shearly, L. F. Eastman, and T. J. Eustis, Journal of Vacuum Science & Technology B, **17,** 1252-4, (1999).
9. J. P. Benedict, R. M. Anderson, and S. J. Klepeis, in *Proceedings of the Twenty-Eighth Annual Technical Meeting of the International Metallographics Society*, Albuquerque, NM, USA, 1996 (ASM Int; Materials Park, OH, USA), p. 277-84.
10. R. F. Egerton, *Electron Energy-Loss Spectroscopy in the Electron Microscope*, 2nd ed. (Plenum Press, New York, 1996), p. 485.
11. V. Serin, C. Colliex, R. Brydson, S. Matar, and F. Boucher, Physical Review B, **58,** 5106-15, (1998).
12. A. Ourmazd, D. W. Taylor, J. Cunningham, and C. W. Tu, Physical Review Letters, **62,** 933-6, (1989).
13. M. Yeadon, M. T. Marshall, F. Hamdani, S. Pekin, H. Morkoc, and J. M. Gibson, Journal of Applied Physics, **83,** 2847-50, (1998).
14. S. Abaidia, V. Serin, G. Zanchi, Y. Kihn, and J. Sevely, Philosophical Magazine A, **72,** 1657-70, (1995).
15. M. Katsikini, E. C. Paloura, T. S. Cheng, and C. T. Foxon, Journal of Applied Physics, **82,** 1166-71, (1997).
16. S. D. Mo and W. Y. Ching, Physical Review B, **57,** 15219-28, (1998).
17. R. Brydson, Journal of Physics D, **29,** 1699-708, (1996).